

Suppression of hPOT1 in Diploid Human Cells Results in an hTERT-Dependent Alteration of Telomere Length Dynamics

Richard Possemato, Jamie C. Timmons, Erica L. Bauerlein, et al.

Mol Cancer Res 2008;6:1582-1593.

Updated version Access the most recent version of this article at:
<http://mcr.aacrjournals.org/content/6/10/1582>

Cited Articles This article cites by 64 articles, 16 of which you can access for free at:
<http://mcr.aacrjournals.org/content/6/10/1582.full.html#ref-list-1>

Citing articles This article has been cited by 4 HighWire-hosted articles. Access the articles at:
<http://mcr.aacrjournals.org/content/6/10/1582.full.html#related-urls>

E-mail alerts [Sign up to receive free email-alerts](#) related to this article or journal.

Reprints and Subscriptions To order reprints of this article or to subscribe to the journal, contact the AACR Publications Department at pubs@aacr.org.

Permissions To request permission to re-use all or part of this article, contact the AACR Publications Department at permissions@aacr.org.

Suppression of hPOT1 in Diploid Human Cells Results in an hTERT-Dependent Alteration of Telomere Length Dynamics

Richard Possemato,¹ Jamie C. Timmons,¹ Erica L. Bauerlein,¹ Naoya Wada,¹ Amy Baldwin,² Kenkichi Masutomi,⁴ and William C. Hahn^{1,3}

¹Department of Medical Oncology, Dana-Farber Cancer Institute and Department of Medicine, Brigham and Women's Hospital and Harvard Medical School; ²The Channing Laboratory, Brigham and Women's Hospital and Department of Medicine, Harvard Medical School, Boston, Massachusetts; ³Broad Institute of Harvard and Massachusetts Institute of Technology, Cambridge, Massachusetts; and ⁴National Cancer Center, Cancer Stem Cell Project, Tokyo, Japan

Abstract

POT1 is a 3' telomeric single-stranded overhang binding protein that has been implicated in chromosome end protection, the regulation of telomerase function, and defining the 5' chromosome terminus. In human cancer cells that exhibit constitutive hTERT activity, hPOT1 exerts control over telomere length. Primary human fibroblasts express low levels of catalytically active hTERT in an S-phase–restricted manner that fails to counteract telomere attrition with cell division. Here, we show that diploid human fibroblasts in which hPOT1 expression has been suppressed harbor telomeres that are longer than control cells. This difference in telomere length delays the onset of replicative senescence and is dependent on S-phase–restricted hTERT expression. These findings are consistent with the view that hPOT1 promotes a nonextendable telomere state resistant to extension by S-phase–restricted telomerase. Manipulating this function of hPOT1 may thus hasten the cytotoxic effects of telomerase inhibition. (Mol Cancer Res 2008;6(10):1582–93)

Introduction

Telomeres are nucleoprotein complexes that cap the termini of eukaryotic chromosomes (1). Mammalian telomeres contain several thousand base pairs of TTAGGG repeats and end in a several hundred base pair 3' extension of the G-rich strand that is required for the formation of a t-loop structure (2). Telomerase is a ribonucleoprotein reverse transcriptase composed

of a catalytic protein subunit, TERT, and a RNA subunit, *TERC*, which together synthesize additional telomeric repeats (3-5). Dyskerin, a RNA-binding molecule that participates in ribonucleoprotein assembly, is associated with catalytically active telomerase (6) and several other proteins have been reported to be associated with telomerase (7). In normal human cells, telomerase activity is tightly regulated. Although *TERC* is expressed constitutively in most cells, hTERT expression is restricted to low levels in S phase of the cell cycle in most diploid nonmalignant cells (8). This low-level hTERT expression fails to maintain telomere length in such cells, and approximately 30 to 100 bp of telomeric DNA are lost per cell division (9). However, it is unclear whether this inability to maintain telomere length is because this low level of hTERT is not competent to act on telomeres or because of a suppressive mechanism inhibiting telomerase action at telomeres in these cells.

Normal human cells reach a replicative limit characterized by entrance into a growth-arrested state termed replicative senescence, which can be triggered in part by dysfunctional telomeres (10). In these cells, entry into replicative senescence requires intact p53 or pRB cell cycle checkpoints (11, 12). In contrast, most immortalized and transformed cells exhibit constitutively high levels of telomerase activity, which correlates with stable telomere length (3, 13). This observation suggests that telomerase activation in premalignant cells results in an immortalized state that is required for tumorigenesis. In support of this hypothesis, overexpression of hTERT facilitates cell immortalization (14), whereas inhibition of telomerase either genetically or pharmacologically in already immortal cancer cell lines results in loss of telomeric sequences, a loss of proliferative capacity, and the onset of crisis (15-17). Consistent with the view that telomerase activation plays an important role in facilitating human cell transformation, coexpression of hTERT with cooperating oncogenes, such as the SV40 large T and small T antigens and RAS, generates tumorigenic cells (18).

Telomere homeostasis is regulated by a multiprotein complex known as the telosome/shelterin complex (19). The results from studies focused on the control of telomere length by telomere-binding proteins suggest that such proteins make up a binary switch that controls whether a telomere is in an extendable or nonextendable state (20). In their initial studies

Received 2/6/08; revised 5/16/08; accepted 6/19/08.

Grant support: NIH National Institute on Aging grant R01 AG23145 and Johnson and Johnson Focused Giving Program Award. R. Possemato was supported by a Howard Hughes Predoctoral Fellowship.

The costs of publication of this article were defrayed in part by the payment of page charges. This article must therefore be hereby marked *advertisement* in accordance with 18 U.S.C. Section 1734 solely to indicate this fact.

Note: Supplementary data for this article are available at Molecular Cancer Research Online (<http://mcr.aacrjournals.org/>).

Requests for reprints: William C. Hahn, Dana-Farber Cancer Institute, 44 Binney Street, Boston, MA 02115. Phone: 617-632-2641; Fax: 617-632-4005. E-mail: william_hahn@dfci.harvard.edu

Copyright © 2008 American Association for Cancer Research.
doi:10.1158/1541-7786.MCR-08-0070

in *Schizosaccharomyces pombe*, Baumann and Cech (21) identified POT1 as a novel telomere-binding protein and a component necessary for the maintenance of a stable telomere. Subsequent genetic and biochemical studies have identified a role for POT1 in telomere length maintenance and telomere capping (22). Overexpression of full-length or alternatively spliced hPOT1 (23) or suppression of *hPOT1* by short hairpin RNA (shRNA; refs. 24, 25) in the telomerase-positive cell line HT1080 led to telomere elongation, whereas overexpression of mutant forms of hPOT1 lacking the 5' oligonucleotide-binding fold domains led to telomere elongation in HTC75/HT1080 cells (22, 26). Recently, a POT1-interacting protein, TPP1, has been identified, which regulates localization of POT1 to the telomere (25, 26) and mediates telomere length control in concert with POT1 (27-29).

In primer extension assays, the ability of POT1 to regulate telomere addition to artificial substrates depended on primer composition. Primers that can fold into telomerase inaccessible G-quadruplex structures were resolved by the addition of POT1 and led to an increase in extension from these primers (30). Alternatively, extension from shorter primers was inhibited by POT1 (31, 32), but elongation, when it occurred, did so with increased processivity (32).

Unlike humans, two very similar POT1 genes, *POT1a* and *POT1b*, are present in mice (33). Two groups have reported that targeted deletion of *POT1a* results in embryonic lethality in the mouse; however, these groups found both telomere elongation (34) and no change in overall telomere length (35) after germline deletion of *POT1a*. In contrast, targeted deletion of *POT1b* fails to change overall telomere length but results in *mTERC*-independent 3' overhang lengthening (35).

Despite these extensive studies into the biology of POT1, the role of hPOT1 in regulating telomerase and telomere length in primary human cells or in cells lacking hTERT is currently unknown. Here, we explored the consequences of suppressing *hPOT1* under conditions where *hTERT* was constitutively expressed, S-phase restricted, or suppressed. We found that suppression of *hPOT1* alters the dynamics of telomere length control in an hTERT-dependent manner. These observations have implications for the timing of the entry of these cells into replicative senescence.

Results

Telomere Length Dynamics of Primary Human Fibroblasts

To understand the role of hPOT1 in telomere length control in primary human cells, we generated lentiviral vectors coexpressing a puromycin or neomycin selectable marker and a shRNA that targets all known *hPOT1* splice variants (hPOT1sh #1 puro and hPOT1sh #1 neo) or a shRNA that targets an unrelated sequence (CONsh puro or CONsh neo) and introduced these shRNAs into mortal BJ human fibroblasts. Expression of either hPOT1sh #1 puro or hPOT1sh #1 neo induced a 75% decrease in the expression of hPOT1 as assessed by quantitative reverse transcription-PCR (RT-PCR) or immunoblotting (Fig. 1A).

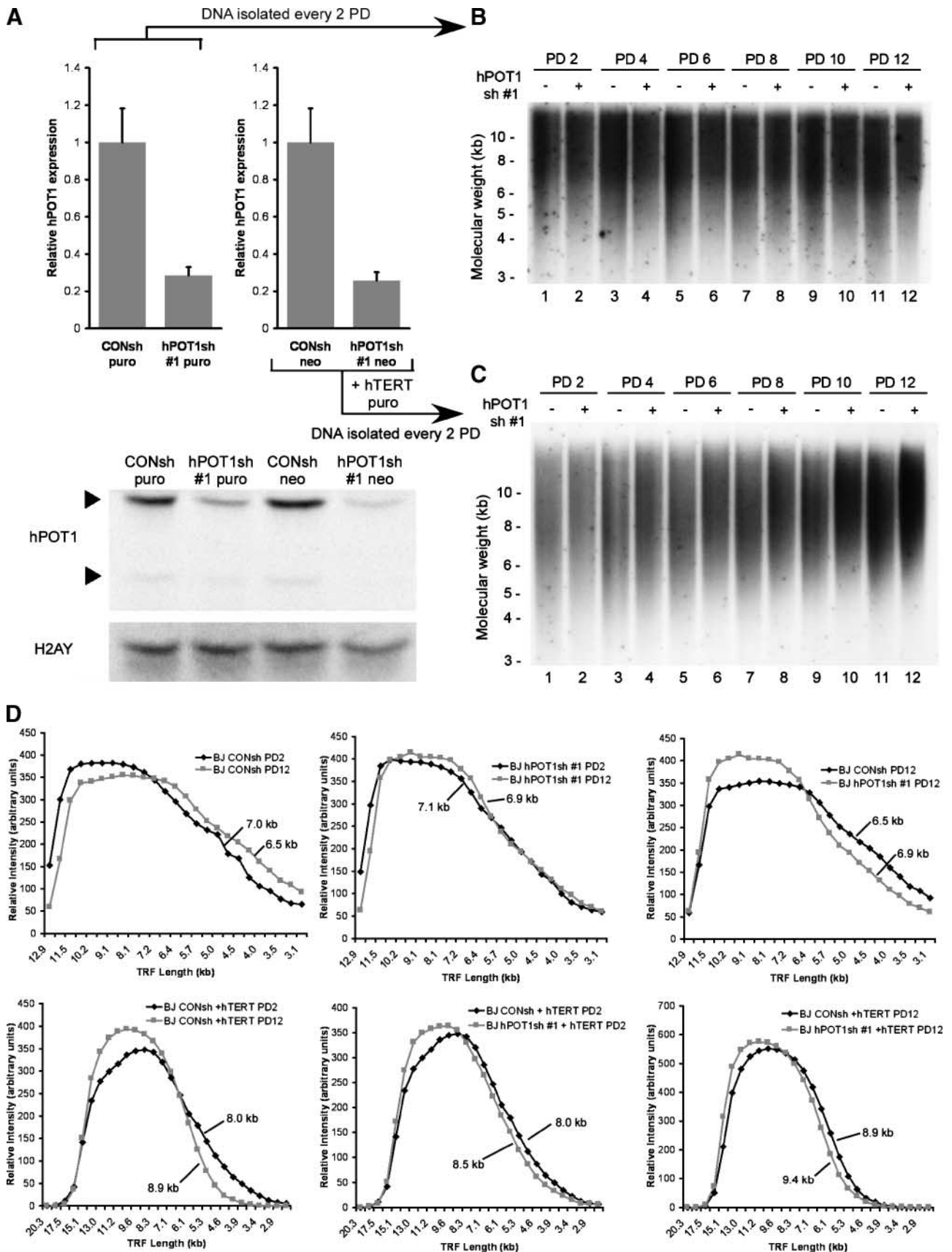
To determine if suppressing hPOT1 expression and overexpressing hTERT in diploid fibroblasts resulted in an increased rate of telomere lengthening, we then infected BJ cells expressing CONsh neo or hPOT1sh #1 neo with a retrovirus encoding

the *hTERT* cDNA (BJ CONsh+ hTERT and BJ hPOT1sh #1+ hTERT). Genomic DNA was isolated from these four cell lines (BJ CONsh, BJ hPOT1sh #1, BJ CONsh+ hTERT, and BJ hPOT1sh #1+ hTERT) every two population doublings (PDs) following infection and analyzed by telomere restriction fragment (TRF) Southern blotting to determine mean TRF length. In consonance with prior reports (9, 14), the mean telomere length decreased by 41 bp/PD in BJ CONsh cells, whereas BJ CONsh+ hTERT cells exhibited overall telomere lengthening of 101 bp/PD (Fig. 1B and C, *odd lanes*). We noted a uniform decrease in TRF length in the BJ CONsh cell population, characterized by an increase in the signal of shorter fragments (compare Fig. 1B, *lanes 1* and *11* and see Fig. 1D, *top left*). When hTERT was expressed constitutively at high levels, we observed that the shortest TRFs increased in size rather than a uniform lengthening of telomeres of all lengths (compare Fig. 1C, *lanes 1* and *11* and see Fig. 1D, *bottom left*) as has been described in murine cells (36).

Surprisingly, we observed an altered telomere shortening dynamic in BJ cells in which *hPOT1* had been suppressed. Over the time course of this experiment, we detected relatively little change in the abundance of shorter TRFs (compare Fig. 1B, *lanes 2* and *12* and see Fig. 1D, *top middle*). Consequently, when compared with control cells, the rate of telomere shortening in BJ hPOT1sh #1 cells was reduced by 52% to 20 bp/PD (Fig. 1B). After 12 PDs, this difference in the rate of telomere attrition results in a 400-bp increase in mean TRF length between BJ hPOT1sh #1 and BJ CONsh cells (compare Fig. 1B, *lanes 11* and *12* and see Fig. 1D, *top right*). Specifically, BJ CONsh cells exhibited stronger signals for TRF fragments shorter than 7 kb (Fig. 1D, *top right*).

We found that either suppressing *hPOT1* or overexpressing hTERT resulted in a smaller proportion of shorter TRF fragments with a corresponding greater proportion of longer fragments (compare Fig. 1C, *lanes 1* and *11* for BJ CONsh+ hTERT cells and Fig. 1B, *lanes 11* and *12* for BJ hPOT1sh #1 cells and see Fig. 1D, *bottom left* and *top right*). Cells in which both *hTERT* was overexpressed and *hPOT1* was suppressed exhibited a 400-bp difference in telomere length within two PDs after introduction of *hTERT* compared with cells overexpressing *hTERT* alone (compare Fig. 1C, *lanes 1* and *2* and see Fig. 1D, *bottom middle*). Subsequent telomere elongation proceeded at the same rate in both populations, and thus, BJ hPOT1sh #1+ hTERT cells maintained an increased telomere length throughout the course of this experiment (compare Fig. 1C, *lanes 1* and *2* with *lanes 11* and *12* and see Fig. 1D, *bottom middle* and *bottom right*). Taken together, these observations suggest that constitutive expression of *hTERT* and suppression of *hPOT1* likely affect telomere length and/or structure in different ways.

To address the possibility that the observed telomere elongation phenotype was due to an off-target effect of RNA interference, we generated a full-length hPOT1 cDNA that is resistant to hPOT1sh #1 by introducing five nucleotide substitutions that do not change the amino acid coding sequence (hPOT1R). We introduced hPOT1R or a control vector into BJ and BJ hTERT cells (BJ hPOT1R and BJ hTERT hPOT1R). Expression of hPOT1R resulted in hPOT1 overexpression, which persisted after subsequent introduction of hPOT1sh #1, whereas the control vector permitted *hPOT1* suppression after



introduction of hPOT1sh #1 (Fig. 2A). In BJ cells containing a control vector, we again found a statistically significant increase ($P \leq 0.000009$) in TRF length of 230 bp on introduction of hPOT1sh #1 (Fig. 2B). In contrast, in BJ hPOT1R cells, we failed to observe telomere elongation on introduction of hPOT1sh #1 (Fig. 2B), suggesting that the telomere elongation phenotype was not the result of off-target effects of RNA interference.

To determine if suppressing hPOT1 expression in diploid human fibroblasts that overexpress hTERT induced increased telomere length as has been observed in other telomerase-positive human cell lines (24, 25), we suppressed *hPOT1* in BJ hTERT cells and also observed a statistically significant increase ($P \leq 0.000032$) in telomere length that was abolished in cells coexpressing hPOT1R (Fig. 2B and C). The BJ hTERT fibroblasts used in these experiments had been passaged until they had achieved a stable maximum telomere length, allowing us to measure the effects of *hPOT1* suppression on this maximal telomere length set point. Suppression of *hPOT1* in the hTERT-immortalized BJ cells resulted in telomere elongation of ~340 bp beyond the stable maximum length as assessed by TRF Southern blotting (Fig. 2B).

Although the observed differences in telomere length are statistically significant, the differences in telomere length being detected in these experiments are at the limit of sensitivity for TRF Southern blotting. Moreover, the estimation of size of the longest telomere lengths is less precise than that of shorter lengths. To confirm these measurements using a second approach, we used quantitative fluorescence *in situ* hybridization (FISH). This method does not measure subtelomeric repeats, which comprise a much greater fraction of the TRF signal in primary cells (37), and therefore, differences in telomere lengths as a percentage of overall telomere length are expected to be larger using this technique. As expected, when comparing primary BJ cells expressing CONsh with those expressing hPOT1sh #1, we noted an increase in fluorescence of 29%, which was abolished in cells expressing hPOT1R (Fig. 2C). Similarly, when comparing BJ hTERT cells with those expressing hPOT1sh #1, we noted an increase in fluorescence of 5.8%, which was also abolished by expression of hPOT1R (Fig. 2C). Together, these observations show that suppressing *hPOT1* in both mortal and immortal human fibroblasts leads to telomere elongation and telomere maintenance at a new set point.

Effects of Replicative History on the Response of Fibroblasts to hPOT1 Suppression

We found that the introduction of two different *hPOT1* shRNAs into early-passage BJ and BJ hTERT cells increased the

short-term doubling time of the cells by 10% to 20% (Fig. 3A). A previous report showed that suppression of *hPOT1* had no effect on the doubling time of immortal fibroblasts but increased the short-term doubling time of nonimmortal human fibroblasts by approximately 30% to 40% (38). In contrast, others have shown more dramatic effects of *hPOT1* suppression on proliferative rates (24, 39). We speculated that the replicative history of the cells dictated their response to suppression of *hPOT1*.

To test this hypothesis, we obtained freshly isolated human foreskin fibroblasts (HFF) or used the aforementioned BJ fibroblasts. After allowing the cultures to proliferate for 0 to 40 additional PDs, we introduced one of two shRNAs targeting all known splice variants of *hPOT1* (hPOT1sh #1 or hPOT1sh #2) or a control sequence (CONsh). *hPOT1* was suppressed to similar levels in each of these cell populations, although we noted diminished hPOT1 expression in HFF cells that had undergone 40 PDs or BJ cells that had undergone 54 PDs (Fig. 3B). Suppression of *hPOT1* in the HFF and BJ cells that had proliferated for the longest time in culture resulted in a 2- to 4-fold greater increase in doubling time as well as a marked induction in senescence-associated β -galactosidase (SA β -gal) staining (Fig. 3A and C; Supplementary Fig. S1).

Prior work has shown that suppression of *hPOT1* resulted in the appearance of telomere dysfunction-induced foci (TIF; ref. 38). To determine whether TIFs were present in cells in which *hPOT1* has been suppressed, we costained the early- and late-passage BJ cells described above for S15 phosphorylated histone H2AX (γ -H2AX) as a marker of DNA damage and a labeled PNA telomeric probe. We found colocalization of γ -H2AX and telomeric foci in both early- and late-passage cells in which *hPOT1* was suppressed (Fig. 3D and E). Although we observed γ -H2AX staining in control and *hPOT1*-suppressed cells, little to no colocalization with telomeres was detected in cells expressing the control shRNA (Fig. 3D and E). The percentage of cells exhibiting γ -H2AX and telomeric focus colocalization was similar in early- and late-passage BJ cells. However, we also observed DNA bridges in late-passage cells that lack *hPOT1* expression at a frequency of 4% (8 of 200 nuclei; Fig. 3F). Taken together, these observations suggest that suppression of *hPOT1* results in telomere dysfunction in all cells regardless of passaging history. However, early-passage cells are able to tolerate this damage, whereas in later-passage cells suppression of *hPOT1* results in telomere uncapping and the onset of senescence.

Long-term Effects of Suppressing hPOT1 on Telomere Length and Proliferative Life Span

With successive cell divisions, mortal human fibroblasts lose telomere length at the rate of approximately 30 to 50 bp/PD (9).

FIGURE 1. Effects of suppressing hPOT1 on telomere dynamics. **A.** hPOT1 mRNA and protein levels. mRNA levels were determined by quantitative RT-PCR (top) and hPOT1 protein levels by immunoblotting (bottom) in BJ cells expressing either an hPOT1 shRNA (*hPOT1sh #1*) or a control shRNA (CONsh) in lentiviral constructs containing either puromycin (*puro*) or neomycin (*neo*) selection markers. Columns, mean of triplicate experiments; bars, SD. Arrows, hPOT1 isoforms. **B.** TRF Southern blotting of mortal BJ cells with passage. DNA was collected at the indicated PDs after infection with CONsh (–) or hPOT1sh #1 (+). Left, DNA size markers in kb. **C.** TRF Southern blotting of BJ cells that overexpress hTERT with successive passage. DNA was collected at the indicated PD after infection with a retrovirus encoding the hTERT cDNA in cells previously infected with CONsh (–) or hPOT1sh #1 (+). Lanes are numbered 1 to 12 for reference. **D.** Densitometry of selected lanes. The relative intensity at regular TRF length intervals is shown and mean TRF lengths for the entire lane are indicated. Top left, compares **B**, lanes 1 (black diamonds) and 11 (gray squares); top middle, compares **B**, lanes 2 (black diamonds) and 12 (gray squares); top right, compares **B**, lanes 11 (black diamonds) and 12 (gray squares); bottom left, compares **C**, lanes 1 (black diamonds) and 11 (gray squares); bottom middle, compares **C**, lanes 1 (black diamonds) and 2 (gray squares); bottom right, compares **C**, lanes 11 (black diamonds) and 12 (gray squares).

Because cells in which *hPOT1* was suppressed exhibited diminished telomere shortening, we assessed the effects of suppressing *hPOT1* on telomere lengths over extended passage and on replicative life span. We cultured HFF and BJ cells expressing CONsh or hPOT1sh #1 or hPOT1sh #2 and determined telomere length as a function of PD. Although cells in which *hPOT1* was suppressed exhibited a longer mean telomere length over time relative to control cells, both populations eventually showed a reduction in mean telomere length at a similar rate (Fig. 4A and B). This observation contrasts with the decrease in telomere shortening rate seen immediately after suppression of *hPOT1*, suggesting that cells in which *hPOT1* has been suppressed reach a new stable

telomere length set point after which normal telomere attrition occurs.

To assess the effects of *hPOT1* suppression in human fibroblasts on replicative senescence, we assessed the long-term proliferative capacity of BJ or BJ hTERT fibroblasts expressing CONsh or hPOT1sh #1 or hPOT1sh #2. Suppression of *hPOT1* in immortal BJ fibroblasts did not affect proliferative capacity over the course of 100 days (Fig. 4C). However, suppression of *hPOT1* in mortal BJ fibroblasts led to a statistically significant extension of the number of PD required to reach senescence (10 PDs; Fig. 4D). This increase in proliferative capacity correlated with the predicted additional PD possible due to the additional telomere length found in cells in which *hPOT1* was

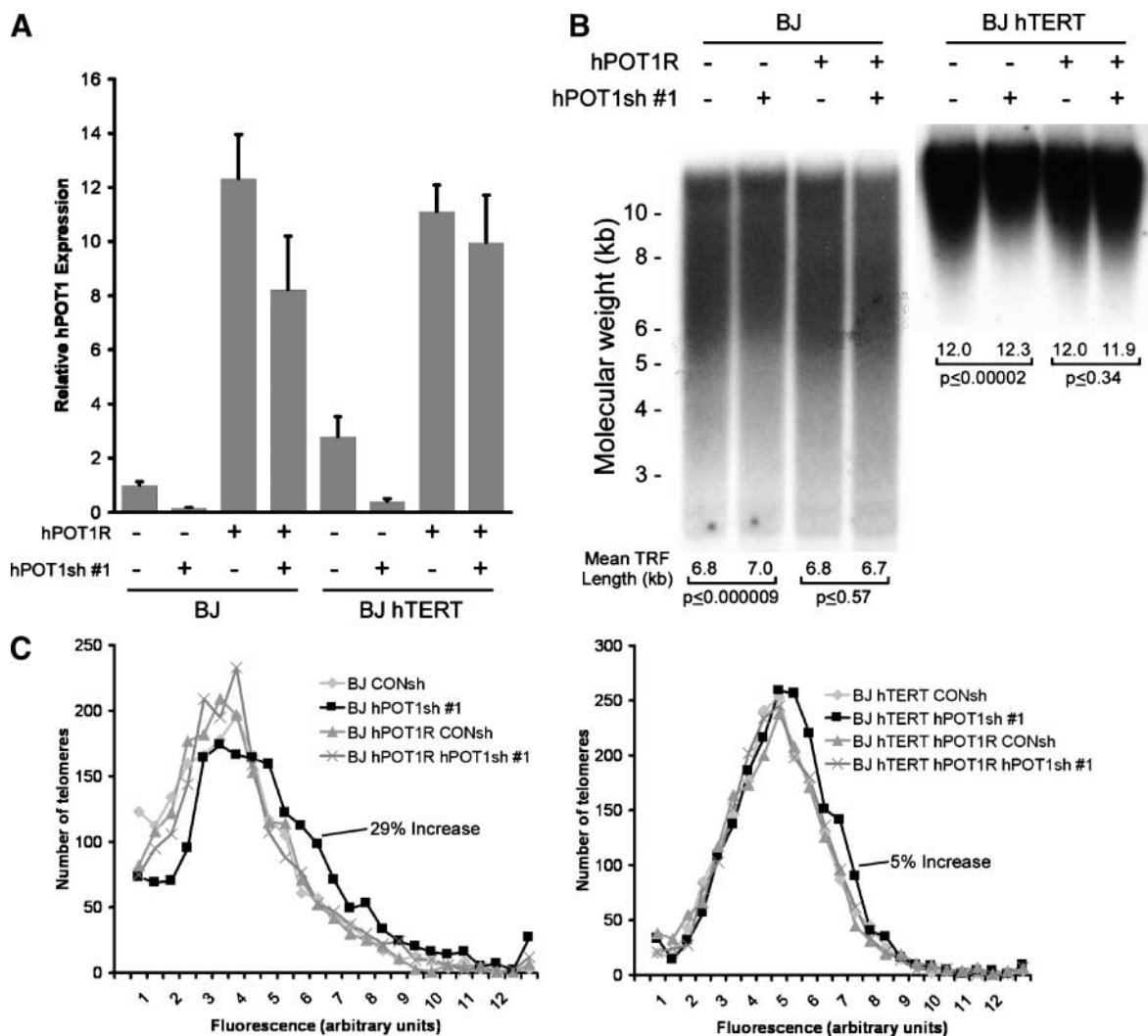
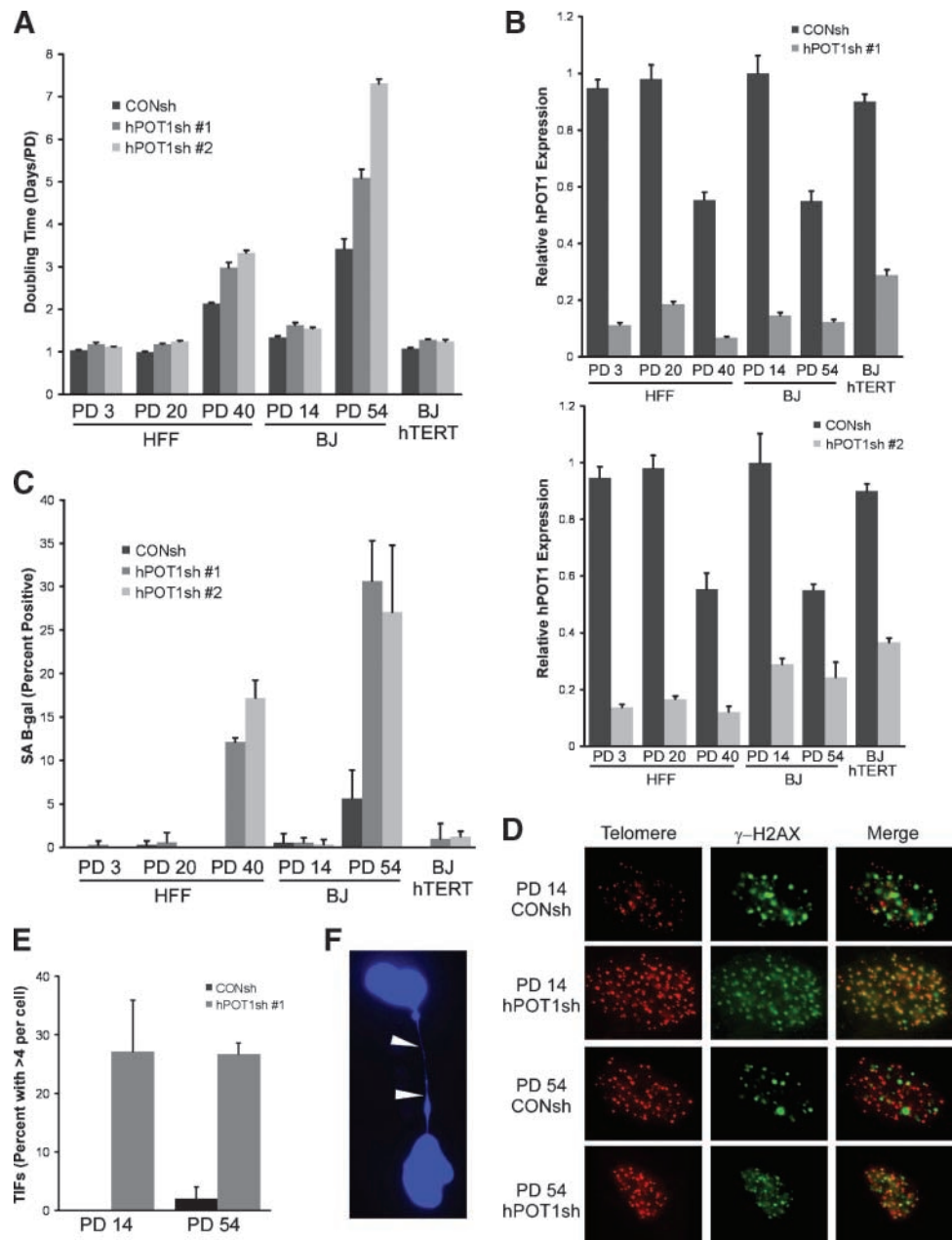


FIGURE 2. Rescue of telomere length changes induced by *hPOT1* suppression. **A.** Overexpression of *hPOT1*. *hPOT1* mRNA levels in BJ or BJ hTERT cells expressing a control hairpin (CONsh) or an *hPOT1* hairpin (hPOT1sh #1) in cells expressing the hPOT1sh #1-resistant version of *hPOT1* (*hPOT1R*). **B.** TRF Southern blotting showing rescue of *hPOT1* suppression. The mean TRF length for each sample taken 10 PDs after infection is indicated beneath the corresponding lane. *P* values (two-tailed *t* test) are shown for the indicated pairwise comparisons from three (BJ) or four (BJ hTERT) replicate experiments. DNA size markers in kb shown on the left are for both gels. **C.** Quantitative telomere FISH showing rescue of *hPOT1* suppression. Results are shown for 12 metaphases for the BJ (left) and BJ hTERT (right) cell lines characterized in **A** and **B**. The fluorescence intensity of telomeres from each sample was assigned into a bin, the intensity of which is indicated on the *X* axis and the number of telomeres contained within that bin is indicated on the *Y* axis. The percent increase in mean fluorescence intensity for the hPOT1sh #1 versus CONsh cell line is indicated. Fluorescence values are arbitrary and cannot be compared between graphs.

FIGURE 3. Short-term effects of *hPOT1* suppression in cells of different proliferative age. **A.** Doubling times of BJ and HFF cells. BJ or HFF cells infected with a control hairpin (*CONsh*) or one of two hairpins targeting *hPOT1* (*hPOT1sh #1* or *hPOT1sh #2*) at the cumulative PD indicated. Doubling times were measured over 13 to 17 d in triplicate. **B.** *hPOT1* mRNA levels in BJ and HFF cells at the indicated PD. Expression of *hPOT1* for cell lines characterized in **A** using primers near the *hPOT1sh #1* (top) or *hPOT1sh #2* (bottom) targeting site. **C.** SA β -gal staining. Values represent the percentage of cells that stained for SA β -gal. For these experiments, at least 100 total cells were scored in triplicate. **D.** TIF images. Staining for γ -H2AX (green) and telomeric DNA (red) are shown from two cells expressing *hPOT1sh #1* that exhibited significant TIF formation and two cells expressing *CONsh* that exhibited little to no TIF formation. **E.** Quantification of TIF formation. Values represent the percentage of nuclei containing more than four foci costaining for γ -H2AX by indirect immunofluorescence and telomeric DNA by PNA FISH. At least 100 nuclei were scored in three independent experiments. **F.** DNA bridge formation. 4',6-Diamidino-2-phenylindole-stained image of a representative DNA bridge (arrows) between two nuclei from PD 54 cells expressing *hPOT1sh #1*. DNA bridges were identified in 4% (8 of 200) of nuclei scored.



suppressed. Consistent with this observation, control cells exhibited a 2-fold increase in SA β -gal staining at an intermediate time point (Fig. 4E). Together, these observations indicated that there is a dichotomous effect of *hPOT1* suppression on human fibroblasts: acute induction of the senescent state in later-passage cells and tolerance and extension in the time to replicative senescence in earlier-passage cells.

Dependence of the Telomere Length Effects of hPOT1 Suppression on hTERT Expression

To determine whether the telomere length phenotype seen in *hPOT1*-suppressed cells is dependent on the presence of S-phase-restricted hTERT, we generated a series of BJ and HFF

cell lines in which we suppressed *hTERT* expression by introducing two different *hTERT*-specific shRNAs (*hTERTsh #1* and *hTERTsh #2*). In BJ cells, we also overexpressed a catalytically inactive mutant of hTERT (DN-hTERT), which we had previously shown to inhibit telomerase activity (15). We confirmed suppression of *hTERT* expression in these cells by RT-PCR and expression of DN-hTERT by immunoblotting (Fig. 5A). We note that suppression of *hTERT* led to an increase in *hPOT1* expression in BJ but not in HFF cells (Fig. 5B). Despite this change in *hPOT1* levels, expression of *hPOT1sh #1* in these cell lines was able to suppress *hPOT1* to similar levels (Fig. 5B).

Analysis of telomere length in both BJ and HFF cells showed that suppression of *hTERT* by shRNA or inhibition

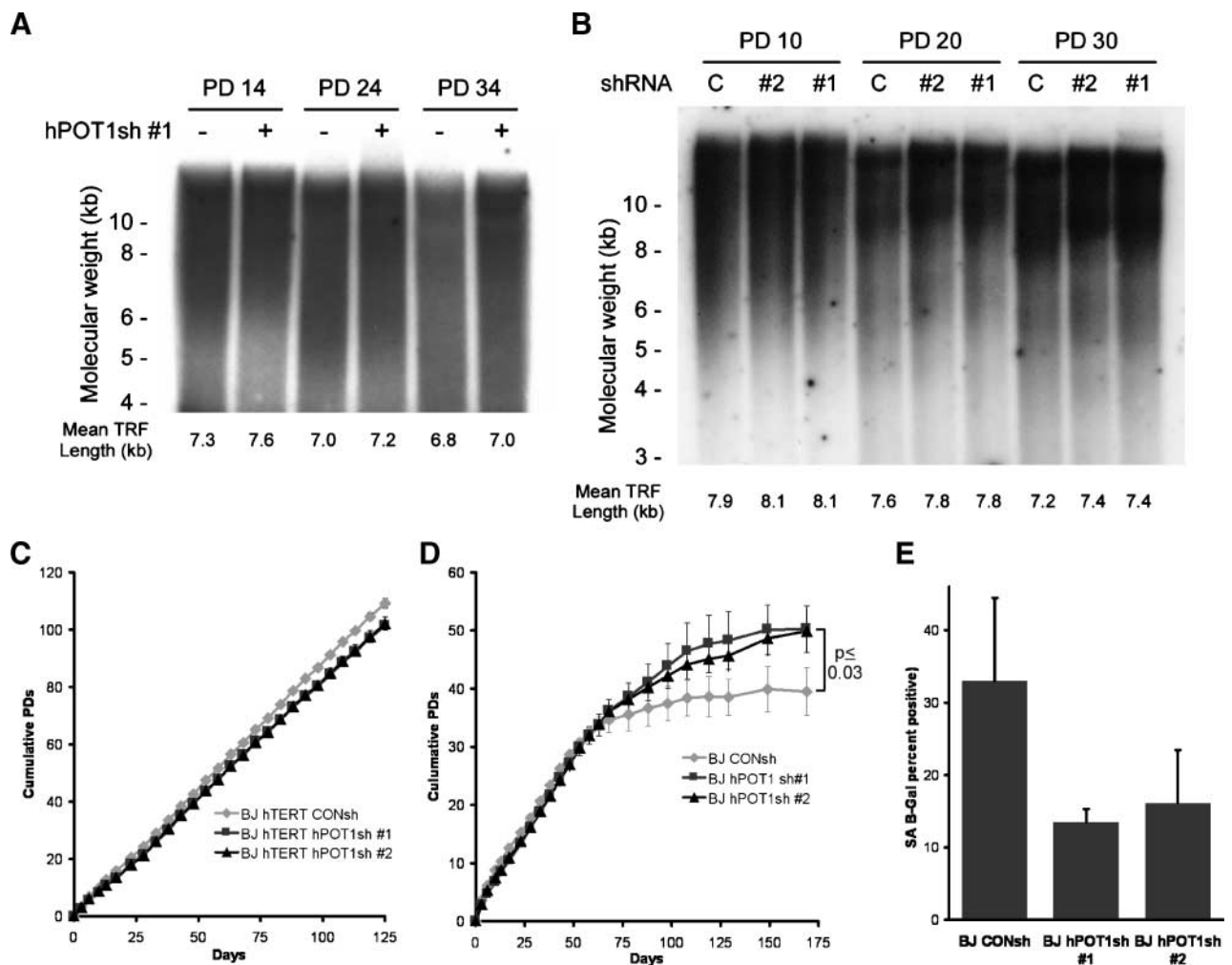


FIGURE 4. Long-term effects of *hPOT1* suppression on telomere length and replicative senescence. **A.** TRF Southern of BJ cells over a span of 34 PDs. BJ cells were infected with a control hairpin (–) or an *hPOT1* hairpin (+) and DNA collected at the indicated mean PD after infection. BJ cells used in this experiment are of a lower initial starting PD from those in Figs. 1 and 2. The mean TRF length for each sample is indicated beneath the corresponding lane. Left, DNA size markers in kb. **B.** TRF Southern of HFF cells over a span of 30 PDs. HFF cells were infected with a control hairpin (C) or one of two *hPOT1*-specific hairpins (#1 or #2) and DNA was collected at the indicated mean PD after infection. The mean TRF length for each sample is indicated beneath the corresponding lane. Left, DNA size markers in kb. **C.** Long-term proliferation of BJ hTERT cells after *hPOT1* suppression. BJ hTERT cells were infected with a control hairpin (CONsh) or one of two *hPOT1* hairpins (*hPOT1* #1 or *hPOT1* #2). Cumulative PD measurements represent an average of three separate cultures. **D.** Long-term proliferation of BJ cells after *hPOT1* suppression. BJ cells were infected with CONsh or *hPOT1* #1 or *hPOT1* #2. Cumulative PD measurements represent an average of three separate cultures and the *P* value (two-tailed *t* test) indicates the degree of statistical significance between the pairwise comparison of CONsh and either *hPOT1* sh #1 or *hPOT1* sh #2 ($P \leq 0.03$, for both comparisons). **E.** SA β -gal staining. Values represent the percentage of positively staining cells of at least 100 total cells scored in triplicate of cells from day 69 of the proliferation experiment shown in **D**.

of telomerase by DN-hTERT diminished the increase in telomere length seen after *hPOT1*sh #1 introduction by 50% to 100% as assessed by TRF length Southern blotting (Fig. 5C) and correlates with results obtained in BJ cells using quantitative FISH (Fig. 5D). These observations indicate that the telomere elongation observed after *hPOT1* suppression depends on the presence of telomerase.

Discussion

Telomere Length Control by *hPOT1*

Prior reports have described the effects of perturbing *POT1* function on telomere length in murine, galline, and immortal human cells with constitutive telomerase expression (22, 25, 34,

35, 40). Here, we investigated the effects of suppressing *hPOT1* in normal human cells where telomerase activity is tightly regulated and telomeric DNA is lost with each round of cell division, a situation that represents normal human cells. We had previously shown that hTERT is expressed in normal human fibroblasts in an S-phase–restricted manner but that this S-phase–regulated telomerase does not affect overall telomere length (8). Therefore, it is unclear whether the inability of hTERT to maintain telomere length is because this low level of hTERT is not competent to act on telomeres or because of a suppressive mechanism inhibiting telomerase in these cells. Studies in *Saccharomyces cerevisiae* further suggest that telomere elongation by telomerase is dependent on telomere length and binding to Rif1 and Rif2 (20) or binding to Rap1p

(41). These observations have led to the view that S-phase telomerase is restricted from elongating telomeres in mortal human cells due to a repressive mechanism located at the telomere.

Here, we present evidence that suppression of *hPOT1* expression by shRNA in mortal diploid human cells altered normal telomere attrition, resulting in a larger mean telomere length in cells in which *hPOT1* has been suppressed. This change in telomere attrition occurred shortly after *hPOT1* suppression, resulting in telomere maintenance at a new set point. Once this new set point was reached, telomere attrition continued to occur at a normal rate with subsequent successive cell divisions.

We and others (22, 23, 25) have observed that suppression of *hPOT1* in immortal cells that express telomerase constitutively leads to an increase in telomere length beyond the normally maintained set point. Here, we find that simultaneous overexpression of *hTERT* and suppression of *hPOT1* in mortal BJ cells results in the combined effect of telomere elongation expected after *hTERT* overexpression in primary cells and the additional increase in telomere length noted after *hPOT1* suppression. However, we noted neither a synergistic nor epistatic relationship between *hTERT* overexpression and *hPOT1* suppression, suggesting that these manipulations may affect telomere length and/or structure in separate, noncomplementary ways.

In normal human fibroblasts that express low levels of hTERT in S phase, we observed that the increase in mean telomere length seen after *hPOT1* suppression can be blunted by suppression of *hTERT* or inhibition of telomerase. These observations suggest that the S-phase-restricted hTERT present in normal human cells is competent to act on the telomere but is inhibited by an hPOT1-dependent suppressive mechanism. However, because we were unable to completely eliminate the telomere elongation phenotype seen in these cells by suppressing hTERT expression, it remains possible that hPOT1 also participates in hTERT-independent telomere replication. Indeed, an increase in homologous recombination has been observed on deletion of *POT1a* in mice (33), and this increased recombination activity may also help explain the telomere lengthening observed here.

Although this study is unique in its analysis of the effects of suppression of hPOT1 on telomere length and replicative senescence in primary human cells and the dependence of these effects on hTERT, our studies are consistent with prior studies in human, murine, and galline cells that constitutively express hTERT. Suppression of POT1 in telomerase-positive human (24, 25, 42) or galline cells (40) induces telomere elongation, and overexpression of an hPOT1 mutant lacking the 5' oligonucleotide-binding fold domains leads to telomere elongation in immortal human cells (22, 26). However, others have found that hPOT1 overexpression in human cells that constitutively express hTERT can promote telomere elongation (23). Furthermore, in mice, two groups have found both telomere elongation (34) or no change in overall telomere length (35) after germ-line deletion of *POT1a*, whereas targeted deletion of *POT1b* results in mTERC-independent 3' overhang lengthening (35). These manuscripts represent a growing body of literature supporting the notion that POT1 functions in telomere 3' overhang protection, telomeric DNA damage signaling, and cell cycle progression. However because many

of the conclusions about POT1 function vary depending on the model system used, we believe that studies in primary human cells are well positioned for understanding the role of hPOT1 in normal human biology.

Contributions to Replicative and Stress-Induced Senescence

Human cells that undergo extensive passage *in vitro* eventually enter a metabolically active yet growth-arrested state termed replicative senescence (43). In normal human cells, telomere attrition occurs with serial passage (9) and has been suggested to trigger the onset of replicative senescence (11). We found that suppression of *hPOT1* in early-passage BJ fibroblasts resulted in a population of cells with a longer mean telomere length that correlates with an increase in the number of PD required to reach replicative senescence.

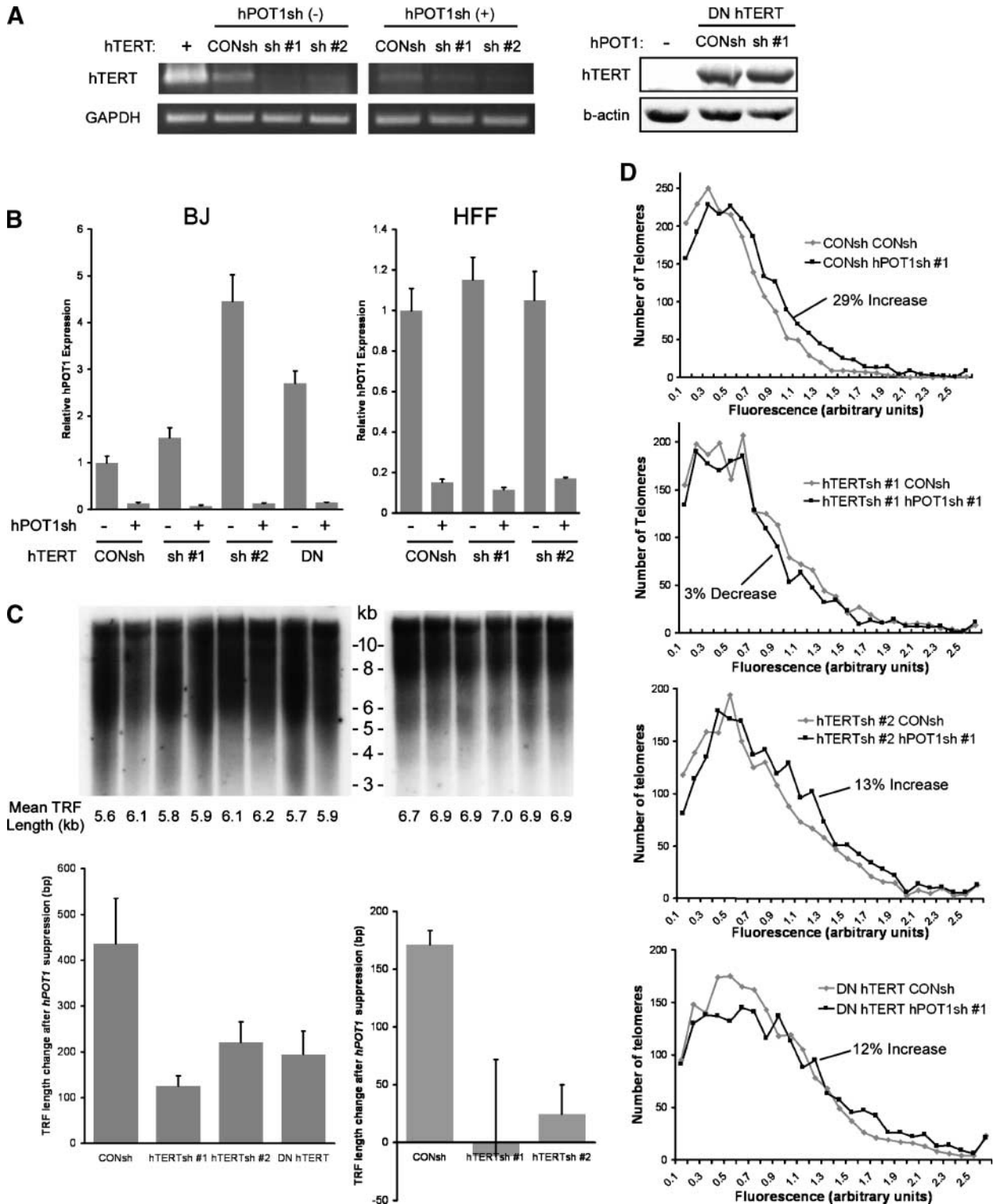
Human cells can also be induced to enter senescence acutely by exposure to stresses such as oncogenic RAS (44), hydrogen peroxide (45), and X-ray irradiation (46). Moreover, when human cells reach replicative senescence, DNA damage response factors accumulate at telomeres in telomere TIFs (47, 48). Suppression of *hPOT1* in human fibroblasts induces TIF formation acutely in both primary and hTERT-overexpressing cells but has been shown to induce ATR-dependent senescence only in primary cells (38, 40, 42, 49, 50). Here, we show that the impairment of cell proliferation seen with *hPOT1* suppression correlates with the proliferative history of primary BJ and HFF cells. Indeed, suppression of *hPOT1* only induces senescence acutely in fibroblasts that have undergone a considerable number of PDs. These observations are consistent with recent reports implicating proliferative age and/or levels of p16, which rise with passage, as key factors in the competency of cells to undergo acute senescence programs (51, 52). Alternatively, it is also possible that changes in telomere structure occur with successive passage that alters the response to suppression of *hPOT1*. In this case, one might expect that late-passage cells are more dependent on hPOT1 for telomere end protection and acutely enter senescence in its absence. Indeed, although we observed induction of TIFs on *hPOT1* suppression in both early- and late-passage cells, we detected DNA bridges only in later-passage cells. These data suggest that early-passage cells are able to tolerate or compensate for reduced hPOT1 expression, whereas in later-passage cells suppression of *hPOT1* results in telomeric damage and the onset of senescence. However, given the number of stimuli that are acting on any given cell, a combination of telomeric and nontelomeric stresses may contribute to the senescence phenotype seen here.

Regulation of the telomere and induction of senescence are emerging as key processes underlying our ability to understand the development of cancer and the process of aging. The recent identification of senescent cells in premalignant and malignant human tissue highlights the importance of understanding the contributions of senescence to the suppression or progression of the malignant state (53). Telomeric stability and proper control of telomere length both are important in determining whether a cell enters the senescent state and are fundamental functional acquisitions found in cancer.

The multiple effects of suppression of *hPOT1* on telomere length control, cellular proliferation, induction of senescence,

and the timing of the onset of replicative senescence provide additional insight into the interplay between telomere biochemistry and the senescence program. One approach to target telomeres involves agents that act by stabilizing G-quadruplex structures (54). Telomeric G-quadruplexes intro-

duce kinks in telomeric DNA and inhibit telomere elongation; therefore, stabilization of G-quadruplexes would be expected to limit cell growth (55, 56). Biochemical studies show that hPOT1 can enhance the ability of G-quadruplex telomeric DNA to act as a telomerase substrate *in vitro* (30). Taken



together, these observations suggest that targeting hPOT1 has the potential to complement the effects of G-quadruplex chemotherapeutics. The observations made in this study provide insight into how such targeting of hPOT1 may affect normal human cells.

Materials and Methods

Cell Culture and Lentiviral and Retroviral Constructs

Culture conditions and retroviral infections were done as described (18, 57, 58). HFFs were isolated from human neonatal foreskin by dispase-mediated separation of the dermis from the epidermis. HFFs from passage 2 were labeled as PD 0. The following sequences were used in the previously described (58) lentiviral vector pLKO.1-puro: CONsh, 5'-ggccccgaagct-gaccctgaagtcacat-3'; hPOT1sh #1, 5'-cggagcatgattcttctaaa-3'; and hPOT1sh #2, 5'-taagtgtctgcatcaagctaca-3'. The puromycin selection cassette was replaced with a neomycin selection cassette in specified vectors. Infections were done at the minimal titer required to achieve ~100% infection efficiency to ensure that simultaneously infected cultures had undergone the same number of PD. Retroviral constructs encoding a control hairpin or *hTERT*-specific hairpins (8) and the DN-*hTERT* (15) construct are as described. The hPOT1R cDNA construct was generated by PCR cloning from pET14-Pot1 (kindly provided by Joachim Lingner, Swiss Institute for Experimental Cancer Research, Epalinges, Switzerland) into pBabe-neo using primers introducing five silent mutations (in capitalized, bold letters) into this hPOT1 cDNA [hPOT1R, 5'-cggagc**TAG**Cttct**G**taaaggtatgg-3' (forward) and 5'-agaaa**GCTA**gctccgctcactctgct-3' (reverse)] as well as two other gene-specific primers [hPOT1, 5'-acaggatccatgcttgggtccagca-3' (*Bam*HI, forward) and 5'-gctaaagctgacggcaatattagatta-3' (*Sall*I, reverse)]. The resulting cDNA was fully sequenced.

Immunoblotting and RT-PCR

Immunoblotting for hPOT1 and H2AY was done by isolating nuclear extracts as follows: cells were scraped into PBS, pelleted (1,000 × *g*, 5 min), resuspended in harvest buffer [10 mmol/L HEPES (pH 7.9), 50 mmol/L NaCl, 0.5 mol/L sucrose, 0.1 mmol/L EDTA, 0.5% Triton, Roche Mini complete protease inhibitor], and incubated on ice for 5 min. Nuclei were pelleted (1,000 × *g*, 10 min), washed in buffer A [10 mmol/L HEPES (pH 7.9), 10 mmol/L KCl, 0.1 mmol/L EDTA, 0.1 mmol/L EGTA], and pelleted again, and the pellet was lysed in buffer C [10 mmol/L HEPES (pH 7.9), 500 mmol/L NaCl, 0.1 mmol/L EDTA, 0.1 mmol/L EGTA, 0.1% NP40, Roche Mini complete protease inhibitor]. This nuclear lysate was sonicated (10 s), and protein concentration was determined

by Lowry assay (Bio-Rad), subjected to electrophoresis (100 μg), and transferred to nitrocellulose (Hybond ECL, Amersham). Guanidine denaturation was done as described (22) before hPOT1 (rabbit polyclonal antibody 978; kindly provided by Titia de Lange, Rockefeller University, New York, NY) and H2AY (Upstate Biotechnology) antibody incubation. Antibodies specific for hTERT (Epitomics) and actin (Sigma) were used as described by the suppliers. The following primer pairs were used for quantitative RT-PCR and RT-PCR: hPOT1 #1, 5'-catacctgcactcaagca-3' and 5'-ccaagatggaaatggtgcc-3'; hPOT1 #2, 5'-tatccgtggtggaatgctt-3' and 5'-gctcaaacaggaaggt-gag-3'; glyceraldehyde-3-phosphate dehydrogenase, 5'-gaaggt-gaaggtcggagctca-3' and 5'-gacaagctcccgttctcag-3'; and hTERT (LT5 and LT6; ref. 59). Quantitative RT-PCR was done in triplicate using SYBR Green Master Mix (ABI 7300; Applied Biosystems). C_t values were determined using ABI Prism software that includes automatic background correction and threshold selection. RT-PCR for hTERT was done as described (8). Briefly, cells were synchronized in S phase by contact inhibition and serum starvation for 48 to 72 h before release into serum-containing medium for 21 h (CONsh) or 18 h (hPOT1sh #1). RT-PCR was done using a one-step RT-PCR kit (SuperScript III, Invitrogen).

Analysis of Telomere Length

Telomere FISH was done as described (60). Twelve metaphases from colcemid-treated (Sigma) cultures were imaged, and compared samples were imaged in the same microscopy session using the same exposure time. Telomeres were identified and fluorescence intensity was measured using CellProfiler⁵ software (61). Telomeres of the same relative fluorescence were binned and the number of telomeres in each bin was reported. The percentage change was determined by comparing average telomere intensity for the two populations tested. TRF Southern blotting was done as described (9) and mean TRF length was measured as described (62) using 0.5% agarose gels. The program ImageJ⁶ was used to quantify signal intensity of the images shown in which the blank area (~6 cm) above the gel was cropped. *P* values of replicate experiments were determined by Student's paired two-sided *t* test using the increase in TRF length for the compared cell lines as input. Telomere lengthening and shortening rates are the slope of a linear regression of a plot of TRF length versus PD.

⁵ <http://cellprofiler.org>

⁶ <http://rsb.info.nih.gov/ij/index.html>

FIGURE 5. Effects of telomerase inhibition on hPOT1-dependent telomere lengthening. **A.** Inhibition of telomerase. BJ cells expressing a control hairpin (–) or a hairpin targeting *hPOT1* (+) and either a second control hairpin (CONsh), one of two hairpins targeting *hTERT* (*sh* #1 or *sh* #2), or a dominant-negative *hTERT* cDNA (DN) were analyzed by RT-PCR on RNA from cells synchronized in S phase by serum starvation and release (CONsh, *sh* #1, and *sh* #2) or Western blotting (CONsh and DN). **B.** *hPOT1* mRNA levels. Relative *hPOT1* expression was determined by quantitative RT-PCR on the cell lines described in **A** as well as HFF cell lines expressing a control hairpin (–) or a hairpin targeting hPOT1 (+) as well as CONsh or hTERTsh #1 or hTERTsh #2. **C.** TRF Southern of cells characterized in **A** and **B**. The mean TRF length at 14 PDs after infection for each sample is indicated beneath the corresponding lane. Bar graphs show the change in telomere length after suppression of *hPOT1* in the cell lines indicated. DNA size markers in kb are shown. **D.** Quantitative telomere FISH. Results of 12 metaphases for the BJ cell lines characterized in **A** to **C** are shown. The fluorescence intensity of telomeres from each sample was assigned into a bin, the intensity of which is indicated on the *X* axis and the number of telomeres contained within that bin is indicated on the *Y* axis. The percent increase in mean fluorescence intensity for the hPOT1sh #1 versus CONsh for each pair of cell lines is indicated. Fluorescence values are arbitrary and cannot be compared between graphs.

Proliferation and SA β -Gal

Proliferation assays were done in triplicate using a Coulter Particle Counter every 5 to 10 d for rapidly dividing cultures and every 10 to 20 d for presenescent cultures. PDs were defined as $[\log_2(\text{cells counted/cells plated})]$. *P* values were determined by Student's paired two-sided *t* test. Doubling time was defined as (days/cumulative PDs) over 13 to 17 d. SA β -Gal staining was done as described (63). The proportion of blue cells was determined by counting at least 100 cells from each triplicate well at the indicated time point or four PDs after selection.

Telomere TIFs

Costaining of γ -H2AX and telomeres was done as described (64) with slight modifications. Cells seeded onto #1.5 coverslips were permeabilized [0.5% Triton X-100, 20 mmol/L HEPES (pH 7.9), 50 mmol/L NaCl, 3 mmol/L MgCl_2 , 300 mmol/L sucrose] before fixation. Images were captured on a Nikon Eclipse E800 microscope using a RT Slider Spot camera and a 100 \times Plan Apo oil immersion objective.

Disclosure of Potential Conflicts of Interest

No potential conflicts of interest were disclosed.

Acknowledgments

We thank Richard Maser, Kwok-Kin Wong, Ronald DePinho, James DiCaprio, Curtis Harris, Hans Widlund, Karl Munger, Peter Sicinski, Joanne Brugge, Jesse Boehm, Supriya Jain, and members of the Hahn lab and the Cichowski lab for reagents, equipment, and technical assistance; Titia de Lange and Stephanie Blackwood for the hPOT1 978 antibody; Joachim Lingner and Patrick Reichenbach for the pET14-Pot1 plasmid; and Utz Herbig for assistance with the TIF experiments.

References

- Blackburn EH. Switching and signaling at the telomere. *Cell* 2001;106:661–73.
- Griffith JD, Comeau L, Rosenfield S, et al. Mammalian telomeres end in a large duplex loop. *Cell* 1999;97:503–14.
- Nakamura TM, Cech TR. Reversing time: origin of telomerase. *Cell* 1998;92:587–90.
- Feng J, Funk WD, Wang SS, et al. The RNA component of human telomerase. *Science* New York NY 1995;269:1236–41.
- Greider CW, Blackburn EH. A telomeric sequence in the RNA of *Tetrahymena* telomerase required for telomere repeat synthesis. *Nature* 1989;337:331–7.
- Cohen SB, Graham ME, Lovrecz GO, Bache N, Robinson PJ, Reddel RR. Protein composition of catalytically active human telomerase from immortal cells. *Science* New York NY 2007;315:1850–3.
- Fu D, Collins K. Purification of human telomerase complexes identifies factors involved in telomerase biogenesis and telomere length regulation. *Mol Cell* 2007;28:773–85.
- Masutomi K, Yu EY, Khurts S, et al. Telomerase maintains telomere structure in normal human cells. *Cell* 2003;114:241–53.
- Harley CB, Futcher AB, Greider CW. Telomeres shorten during ageing of human fibroblasts. *Nature* 1990;345:458–60.
- Wright WE, Shay JW. Cellular senescence as a tumor-protection mechanism: the essential role of counting. *Curr Opin Genet Dev* 2001;11:98–103.
- Wright WE, Shay JW. Historical claims and current interpretations of replicative aging. *Nat Biotechnol* 2002;20:682–8.
- Shay JW, Wright WE. Quantitation of the frequency of immortalization of normal human diploid fibroblasts by SV40 large T-antigen. *Exp Cell Res* 1989;184:109–18.
- Kim NW, Piatyszek MA, Prowse KR, et al. Specific association of human telomerase activity with immortal cells and cancer. *Science* New York NY 1994;266:2011–5.
- Bodnar AG, Ouellette M, Frolkis M, et al. Extension of life-span by introduction of telomerase into normal human cells. *Science* New York NY 1998;279:349–52.
- Hahn WC, Stewart SA, Brooks MW, et al. Inhibition of telomerase limits the growth of human cancer cells. *Nat Med* 1999;5:1164–70.
- Herbert B, Pitts AE, Baker SI, et al. Inhibition of human telomerase in immortal human cells leads to progressive telomere shortening and cell death. *Proc Natl Acad Sci U S A* 1999;96:14276–81.
- Zhang X, Mar V, Zhou W, Harrington L, Robinson MO. Telomere shortening and apoptosis in telomerase-inhibited human tumor cells. *Genes Dev* 1999;13:2388–99.
- Hahn WC, Counter CM, Lundberg AS, Beijersbergen RL, Brooks MW, Weinberg RA. Creation of human tumour cells with defined genetic elements. *Nature* 1999;400:464–8.
- de Lange T. Shelterin: the protein complex that shapes and safeguards human telomeres. *Genes Dev* 2005;19:2100–10.
- Teixeira MT, Americ M, Sperisen P, Lingner J. Telomere length homeostasis is achieved via a switch between telomerase-extendible and nonextendible states. *Cell* 2004;117:323–35.
- Baumann P, Cech TR. Pot1, the putative telomere end-binding protein in fission yeast and humans. *Science* New York NY 2001;292:1171–5.
- Loayza D, De Lange T. POT1 as a terminal transducer of TRF1 telomere length control. *Nature* 2003;423:1013–8.
- Colgin LM, Baran K, Baumann P, Cech TR, Reddel RR. Human POT1 facilitates telomere elongation by telomerase. *Curr Biol* 2003;13:942–6.
- Veldman T, Etheridge KT, Counter CM. Loss of hPot1 function leads to telomere instability and a cut-like phenotype. *Curr Biol* 2004;14:2264–70.
- Ye JZ, Hockemeyer D, Krutchinsky AN, et al. POT1-interacting protein PIP1: a telomere length regulator that recruits POT1 to the TIN2/TRF1 complex. *Genes Dev* 2004;18:1649–54.
- Liu D, Safari A, O'Connor MS, et al. PTOP interacts with POT1 and regulates its localization to telomeres. *Nat Cell Biol* 2004;6:673–80.
- Wang F, Podell ER, Zaug AJ, et al. The POT1-TPP1 telomere complex is a telomerase processivity factor. *Nature* 2007;445:506–10.
- Xin H, Liu D, Wan M, et al. TPP1 is a homologue of ciliate TEBP- β and interacts with POT1 to recruit telomerase. *Nature* 2007;445:559–62.
- Chen LY, Liu D, Songyang Z. Telomere maintenance through spatial control of telomeric proteins. *Mol Cell Biol* 2007;27:5898–909.
- Zaug AJ, Podell ER, Cech TR. Human POT1 disrupts telomeric G-quadruplexes allowing telomerase extension *in vitro*. *Proc Natl Acad Sci U S A* 2005;102:10864–9.
- Kelleher C, Kurth I, Lingner J. Human protection of telomeres 1 (POT1) is a negative regulator of telomerase activity *in vitro*. *Mol Cell Biol* 2005;25:808–18.
- Lei M, Zaug AJ, Podell ER, Cech TR. Switching human telomerase on and off with hPOT1 protein *in vitro*. *J Biol Chem* 2005;280:20449–56.
- He H, Multani AS, Cosme-Blanco W, et al. POT1b protects telomeres from end-to-end chromosomal fusions and aberrant homologous recombination. *EMBO J* 2006;25:5180–90.
- Wu L, Multani AS, He H, et al. Pot1 deficiency initiates DNA damage checkpoint activation and aberrant homologous recombination at telomeres. *Cell* 2006;126:49–62.
- Hockemeyer D, Daniels JP, Takai H, de Lange T. Recent expansion of the telomeric complex in rodents: two distinct POT1 proteins protect mouse telomeres. *Cell* 2006;126:63–77.
- Hemann MT, Strong MA, Hao LY, Greider CW. The shortest telomere, not average telomere length, is critical for cell viability and chromosome stability. *Cell* 2001;107:67–77.
- Hultdin M, Gronlund E, Norrback K, Eriksson-Lindstrom E, Just T, Roos G. Telomere analysis by fluorescence *in situ* hybridization and flow cytometry. *Nucleic Acids Res* 1998;26:3651–6.
- Hockemeyer D, Sfeir AJ, Shay JW, Wright WE, de Lange T. POT1 protects telomeres from a transient DNA damage response and determines how human chromosomes end. *EMBO J* 2005;24:2667–78.
- Yang Q, Zheng YL, Harris CC. POT1 and TRF2 cooperate to maintain telomeric integrity. *Mol Cell Biol* 2005;25:1070–80.
- Churikov D, Price CM. Pot1 and cell cycle progression cooperate in telomere length regulation. *Nat Struct Mol Biol* 2008;15:79–84.
- Marcand S, Gilson E, Shore D. A protein-counting mechanism for telomere length regulation in yeast. *Science* New York NY 1997;275:986–90.
- Yang Q, Zhang R, Horikawa I, et al. Functional diversity of human protection

of telomeres 1 isoforms in telomere protection and cellular senescence. *Cancer Res* 2007;67:11677–86.

43. Wei W, Sedivy JM. Differentiation between senescence (M1) and crisis (M2) in human fibroblast cultures. *Exp Cell Res* 1999;253:519–22.
44. Serrano M, Lin AW, McCurrach ME, Beach D, Lowe SW. Oncogenic ras provokes premature cell senescence associated with accumulation of p53 and p16INK4a. *Cell* 1997;88:593–602.
45. Chen QM, Prowse KR, Tu VC, Purdom S, Linskens MH. Uncoupling the senescent phenotype from telomere shortening in hydrogen peroxide-treated fibroblasts. *Exp Cell Res* 2001;265:294–303.
46. Suzuki K, Mori I, Nakayama Y, Miyakoda M, Kodama S, Watanabe M. Radiation-induced senescence-like growth arrest requires TP53 function but not telomere shortening. *Radiat Res* 2001;155:248–53.
47. d'Adda di Fagnana F, Reaper PM, Clay-Farrace L, et al. A DNA damage checkpoint response in telomere-initiated senescence. *Nature* 2003;426:194–8.
48. Takai H, Smogorzewska A, de Lange T. DNA damage foci at dysfunctional telomeres. *Curr Biol* 2003;13:1549–56.
49. Denchi EL, de Lange T. Protection of telomeres through independent control of ATM and ATR by TRF2 and POT1. *Nature* 2007;448:1068–71.
50. Guo X, Deng Y, Lin Y, et al. Dysfunctional telomeres activate an ATM-ATR-dependent DNA damage response to suppress tumorigenesis. *EMBO J* 2007;26:4709–19.
51. Benanti JA, Galloway DA. Normal human fibroblasts are resistant to RAS-induced senescence. *Mol Cell Biol* 2004;24:2842–52.
52. Itahana K, Zou Y, Itahana Y, et al. Control of the replicative life span of human fibroblasts by p16 and the polycomb protein Bmi-1. *Mol Cell Biol* 2003;23:389–401.
53. Sarkisian CJ, Keister BA, Stairs DB, Boxer RB, Moody SE, Chodosh LA. Dose-dependent oncogene-induced senescence *in vivo* and its evasion during mammary tumorigenesis. *Nat Cell Biol* 2007;9:493–505.
54. Patel DJ, Phan AT, Kuryavvi V. Human telomere, oncogenic promoter and 5'-UTR G-quadruplexes: diverse higher order DNA and RNA targets for cancer therapeutics. *Nucleic Acids Res* 2007;35:7429–55.
55. Fletcher TM, Sun D, Salazar M, Hurley LH. Effect of DNA secondary structure on human telomerase activity. *Biochemistry* 1998;37:5536–41.
56. Zahler AM, Williamson JR, Cech TR, Prescott DM. Inhibition of telomerase by G-quartet DNA structures. *Nature* 1991;350:718–20.
57. Morgenstern JP, Land H. Advanced mammalian gene transfer: high titre retroviral vectors with multiple drug selection markers and a complementary helper-free packaging cell line. *Nucleic Acids Res* 1990;18:3587–96.
58. Moffat J, Grueneberg DA, Yang X, et al. A lentiviral RNAi library for human and mouse genes applied to an arrayed viral high-content screen. *Cell* 2006;124:1283–98.
59. Nakamura TM, Morin GB, Chapman KB, et al. Telomerase catalytic subunit homologs from fission yeast and human. *Science New York NY* 1997;277:955–9.
60. Martens UM, Zijlmans JM, Poon SS, et al. Short telomeres on human chromosome 17p. *Nat Genet* 1998;18:76–80.
61. Carpenter AE, Jones TR, Lamprecht MR, et al. CellProfiler: image analysis software for identifying and quantifying cell phenotypes. *Genome Biol* 2006;7:R100.
62. Counter CM, Hahn WC, Wei W, et al. Dissociation among *in vitro* telomerase activity, telomere maintenance, and cellular immortalization. *Proc Natl Acad Sci U S A* 1998;95:14723–8.
63. Dimri GP, Lee X, Basile G, et al. A biomarker that identifies senescent human cells in culture and in aging skin *in vivo*. *Proc Natl Acad Sci U S A* 1995;92:9363–7.
64. Herbig U, Jobling WA, Chen BP, Chen DJ, Sedivy JM. Telomere shortening triggers senescence of human cells through a pathway involving ATM, p53, and p21(CIP1), but not p16(INK4a). *Mol Cell* 2004;14:501–13.